Multi-axial Strength of Metallic Foams and Lattice Materials

Norman A. FLECK

Engineering Department, Cambridge University, Cambridge, CB2 1PZ, UK

Abstract: The multi-axial yield strength of metallic foams and lattice materials is reviewed. It is found that metallic foams have bending-dominated microstructures under all loading states, whereas lattice materials such as the octet-truss can be designed to be stretching-dominated in their response. Consequently, lattice materials have higher stiffness and strengths at a given relative density. The yield surface for metallic foams can be approximated by an ellipse, with isotropic hardening, whereas lattice materials have a series of flats on their yield surface reflecting their periodic architecture. Collapse calculations are reported for sandwich panels: it is shown that the pyramidal truss lattice material has a superior response to that of the tetrahedral core under combined shear and normal loading, and this microstructure is recommended for practical use.

Key words: *metallic foams, lattice materials, octet-truss, sandwich panels, yield surface.*

1. INTRODUCTION

Recently, a number of new architectures of porous metal has become available: *metallic foams* with a stochastic microstructure, and *lattice materials*, such as the octet truss, with a periodic microstructure. Intensive research by a number of international research groups has culminated in the publication of a design guide [1], reviewing both material properties and appropriate design methods. For both architectures, the typical relative density $\overline{\rho}$ is in the range of about 0.05 to 0.3. Experiments reveal that both closed and open cell metallic foams deform by local bending of cell walls and so the Young's modulus of scales with $\overline{\rho}^2$, while the uniaxial strength scales with $\overline{\rho}^{3/2}$ [1]. In contrast, lattice materials undergo local stretching of their cell walls, and so the Young's modulus and uniaxial strength scale linearly with $\overline{\rho}$. Thus, metallic foams have much lower stiffnesses and strengths than lattice materials for a given mass, and are preferable in packaging applications where a low collapse strength is needed in order to prevent excessive accelerations on the protected object. In contrast, lattice materials are preferable in applications requiring high specific stiffness and strength.

2. YIELD SURFACE FOR METALLIC FOAMS

The multi-axial yield surface of two aluminium alloy foams Alporas[1] and Duocel[2] has been measured by performing axisymmetric triaxial cell tests on circular cylindrical specimens. Alporas is a closed cell foam of composition Al-Ca 5 –Ti 4 (wt.%), while the open cell Duocel foam has composition Al6101-T6. A series of proportional and non-proportional loading tests [2] show that the foams are to be approximately isotropic in response. The measured yield surface is found to satisfy the relation,

$$\Phi \equiv \hat{\sigma} - Y \le 0 \tag{1}$$

where we have defined the *equivalent stress* $\hat{\sigma}$ by

$$\hat{\sigma}^2 \equiv \frac{1}{\left(1+(\alpha/3)^2\right)}\left[\sigma_e^{\,2} + \alpha^2 \sigma_m^{\,2}\right] \tag{2}$$

in terms of the von Mises effective stress $\sigma_e \equiv \sqrt{\frac{3}{2} s_{ij} s_{ij}}$ (with s_{ij} as the usual stress deviator) and the hydrostatic stress $\sigma_m \equiv \frac{1}{3}\sigma_{kk}$. This definition gives a yield surface of elliptical shape in $(\sigma_m - \sigma_e)$ space, with a uniaxial yield strength (in tension and in compression) of $\hat{\sigma}$, and a hydrostatic strength of $|\sigma_m| = \frac{\sqrt{1+(\alpha/3)^2}}{\alpha}\hat{\sigma}$. The parameter α defines the aspect ratio of the ellipse: in the limit $\alpha=0$, $\hat{\sigma}$ reduces to σ_e and a J2 flow theory solid is recovered. Two material properties are now involved instead of one: the uniaxial yield strength, Y, and the pressure-sensitivity coefficient, α. The material property Y is measured by a simple compression test, which can also be used to measure α in the way described below. A large amount of data on the yield strength of metallic foams has been collected by Ashby *et al.* [1], and a best-it to the available data shows that Y depends upon the relative density $\overline{\rho}$ according to

$$Y \approx 0.3\overline{\rho}^{3/2}\sigma_Y \tag{3}$$

where σ_Y is the yield strength of the cell wall material.

The yield surfaces for Alporas and Duocel for compressive stress states are shown in Fig. 1.

[1] manufactured by Shinko Wire Company, Amagasaki, Japan

[2] manufactured by ERG, Oakland, CA, USA.

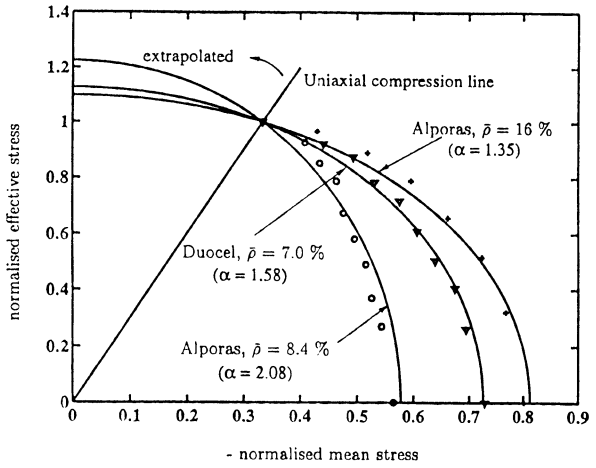

Fig. 1. Initial surfaces for Alporas and Duocel foams. The surfaces are approximately elliptical, and are described adequately by equations Eqs.(1) and (2). The stresses have been normalised by the uniaxial yield strength (0.5 MPa for Duocel, 1.0 MPa for Alporas of $\bar{\rho}$=8.4%, and 2.0 MPa for Alporas of $\bar{\rho}$=16%).

The data have been normalised by the uniaxial compressive yield strength, so that $\sigma_e = 1$ and $\sigma_m = 1/3$ for the case of uniaxial compression. We note that the aspect ratio α of the ellipse lies in the range 1.35 to 2.08. The ratio of hydrostatic strength to shear strength is given by $\sqrt{3}/\alpha$, according to Eq.(2), with a typical value of 0.9 for $\alpha = 2$; thus, metallic foams are highly pressure sensitive in their yield behaviour. The effect of yield surface shape is reflected in the measured plastic Poisson's ratio in a uniaxial compression test: the ratio of transverse strain to axial strain v^P depends upon α. The yield surface shape is sufficiently simple for an analytical expression to be derivable for v^P in terms of α, giving

$$v^P = \frac{\frac{1}{2} - \left(\frac{\alpha}{3}\right)^2}{1 + \left(\frac{\alpha}{3}\right)^2} \tag{4}$$

with the inversion

$$\alpha = 3\left(\frac{\frac{1}{2} - v^P}{1 + v^P}\right)^{1/2} \tag{5}$$

Thus, measurement of v^P in a uniaxial compression test offers a quick and simple method for estimation of the value for α, and thereby the shape of the yield surface. Preliminary experience suggests that the measurement of v^P is best done by compressing a sample, with suitably lubricated loading platens, to a uniaxial strain of 20-30%. Typical values of v^P are in the range 0 to 0.25.

Having defined the yield surface shape, it remains to stipulate how the yield surface evolves with strain. For simplicity, we shall assume that isotropic hardening occurs: the yield surface grows in a geometrically self-similar manner with strain; the limited measurements of the yield surface for metallic foams approximate this [2]. We assume that the strain-hardening rate scales with the uniaxial compression response as follows. The plastic strain-rate is taken to be normal to the yield surface Eq.(1), and specified by

$$\dot{\varepsilon}^P_{ij} = \dot{\hat{\varepsilon}} \frac{\partial \Phi}{\partial \sigma_{ij}} \tag{6}$$

where the equivalent strain-rate $\dot{\hat{\varepsilon}}$ is

$$\dot{\hat{\varepsilon}} = \dot{\hat{\sigma}} / h(\hat{\sigma}) \tag{7}$$

and h is the slope of the true stress versus logarithmic plastic strain curve in uniaxial compression at a stress level $\sigma = \hat{\sigma}$. For the case of uniaxial compression (or tension), the above definitions of $\hat{\sigma}$ and of $\hat{\varepsilon}$ have been so normalised that $\hat{\sigma}$ is the uniaxial stress and $\hat{\varepsilon}$ is the uniaxial plastic strain-rate. An explicit expression for $\dot{\hat{\varepsilon}}$ in terms of the effective strain-rate and mean strain-rate:

$$\dot{\hat{\varepsilon}}^2 \equiv \left(1 + (\alpha/3)^2\right)\left[\dot{\varepsilon}_e{}^2 + \frac{1}{\alpha^2}\dot{\varepsilon}_m{}^2\right] \tag{8}$$

It is emphasised that the model assumes a unique strain hardening response, characterised by the evolution of $\hat{\sigma}$ and its work-conjugate $\hat{\varepsilon}$. Unless otherwise stated, the uniaxial compressive stress-strain response is used to define the $\hat{\sigma} - \hat{\varepsilon}$ relation. Some checks on the accuracy of this approach are given in Fig. 2: The measured tensile, compressive and shear stress-strain curves for 3 densities of Alporas are shown in terms of $\hat{\sigma}$ versus $\hat{\varepsilon}$: the curves almost collapse unto a unique curve up to peak strength.

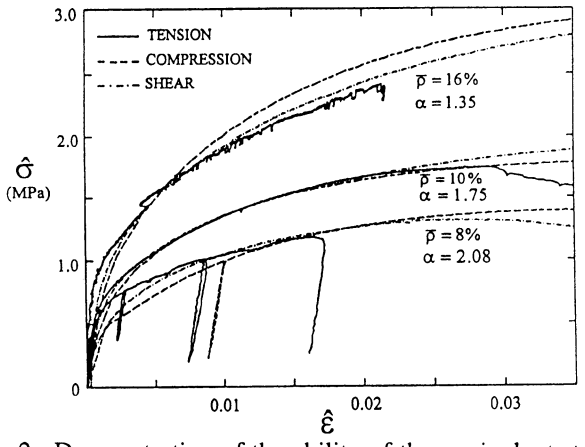

Fig. 2. Demonstration of the ability of the equivalent stress $\hat{\sigma}$ and the equivalent strain $\hat{\varepsilon}$ to define uniquely the stress-strain response of Alporas foams. The tension, compression and shear response are plotted in terms of $\hat{\sigma}$ and $\hat{\varepsilon}$.

The underlying reason why metallic foams have a hydrostatic strength comparable to their shear strength is the presence of various *imperfections* within the microstructure; these include cell wall waviness, fractured and missing cell walls, and cell wall mis-alignment. Whilst the perfect foam would exhibit a hydrostatic strength an order of magnitude greater than the shear strength (with collapse by the stretching of cell walls under hydrostatic loading, and bending under shear loading), only a small degree of imperfection results in the foam deforming by the same mechanism of cell wall bending under all loading states [3], and so the hydrostatic and shear strengths are comparable. The above constitutive model for metallic foams has been implemented within the ABAQUS finite element code, and used with success to predict the structural collapse response of foam-cores sandwich panels [4].

3. MULTI-AXIAL YIELD OF LATTICE MATERIALS

Lattice materials, such as the Buckminster Fuller octet-truss, possess a periodic microstructure in contrast to stochastic foams. Deshpande *et al.* [5] have recently analysed the criteria for the construction of stretching dominated cellular microstructures, with *similarly situated nodes*: nodes are said to be similarly situated if the remainder of the structure appears the same and in the same orientation when viewed from any of the nodes. For such a structure, a necessary and sufficient condition for the structure to be stretching-dominated is that the connectivity at each node is 12 for a 3D structure and 6 for a 2D structure. The octet-truss structure, as shown in Figure 3, has a connectivity of 12 and therefore behaves as a stretching dominated structure, with a stiffness and strength which scales linearly with the relative density.

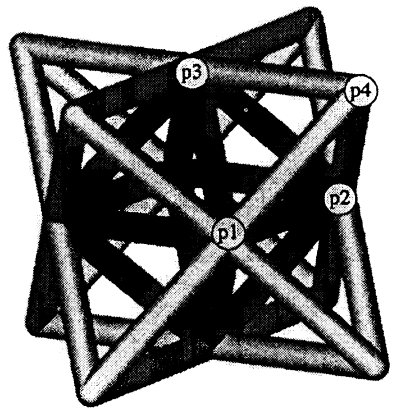

Fig. 3. Structure of the octet-truss lattice material. The darkened struts represent an octahedral cell while the nodes labelled p1-p4 form a tetrahedral cell.

The octet-truss structure has a FCC microstructure, and can be constructed by packing either octahedra or regular tetrahedra, as shown in Fig. 4. Note that the 1-2 plane of Fig. 4 is a close-packed plane of the FCC structure, and constitutes a fully triangulated layer in the lattice material. Thus, the octet-truss material can be constructed by the successive packing of the triangulated layers in the 'ABCABC...' positions with each layer separated by a tetrahedral core.

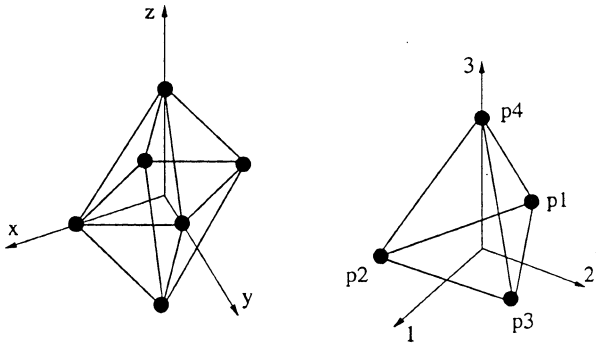

Fig. 4. Isometric sketches of the octahedral and tetrahedral cells with the associated co-ordinate systems.

Consider an octet-truss constructed from identical circular cylindrical struts, each of radius a and length ℓ. Then, the relative density of the octet-truss lattice material (defined by the ratio of the density of the lattice material to the density of the solid material from which it is made) is given by

$$\overline{\rho} = 6\sqrt{2}\pi\left(\frac{a}{\ell}\right)^2 \qquad (9)$$

The yield surface for the octet-truss can be calculated by performing a number of upper bound calculations for the competing collapse modes, see [6]. The microstructure has orthotropic symmetry (x,y,z) as sketched in Fig. 4, and the yield surface can be approximated by the following quadratic expression,

$$\Phi = \frac{4}{9}\left[(\sigma_x-\sigma_y)^2+(\sigma_y-\sigma_z)^2+(\sigma_z-\sigma_x)^2\right]$$
$$+4\left[\sigma_{xy}{}^2+\sigma_{yz}{}^2+\sigma_{zx}{}^2\right]+\sigma_m{}^2-\left[2\sqrt{2}\pi\left(\frac{a}{\ell}\right)\sigma_Y\right]^2=0 \qquad (10)$$

where σ_Y is the uniaxial strength of the fully dense solid, and $2\sqrt{2}\pi\left(\frac{a}{\ell}\right)\sigma_Y$ is the uniaxial yield strength of the octet-truss in a principal direction of orthotropy [6]. Detailed calculations reported in [6] for a large number of collapse modes show that Eq.(10) may over-estimate the collapse strength by as much as a factor of two for certain stress states; however, no improved analytical formula for multi-axial yield of lattice materials is available at present.

4. COMPARISON OF SANDWICH PANEL YIELD FOR A FOAM CORE AND LATTICE MATERIAL CORE

A promising application for both metallic foams and lattice materials is in the core of a sandwich panel. For example, two fully dense face sheets made from high strength aluminium alloy are separated by a foam core in order to achieve high bending stiffness and strength at low mass. The core of such sandwich panels is usually loaded by a combination of transverse shear τ and normal tension σ_n, as sketched in Figure 5, and it is instructive to determine the collapse locus for an arbitrary combination of loading (σ_n, τ).

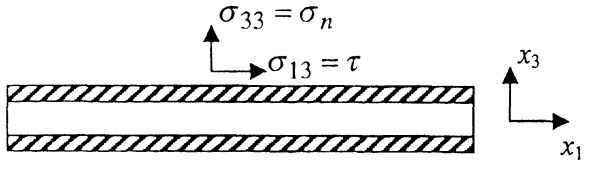

Fig. 5. Sketch of sandwich panel subjected to through thickness shear and to through-thickness direct loading.

This may be done in straightforward manner for the case of a metallic foam, with yield surface given by Eqs.(1) and (2), upon assuming that the face sheets remain elastic and the plastic strains in the core greatly exceed the elastic strains. The in-plane plastic strains vanish due to the constraint of the face-sheets, and normality of plastic flow dictates that the direct in-plane stresses $\sigma_{11} = \sigma_{22}$ within the core satisfies

$$\sigma_{11} = \sigma_{22} = \frac{9 - 2\alpha^2}{9 + 4\alpha^2}\sigma_n \qquad (11)$$

The collapse surface for the foam core follows by substitution of Eq.(11) into Eqs.(1) and (2) to give,

$$3\tau^2 + \frac{24\alpha^4}{\left(9 + 4\alpha^2\right)^2}\sigma_n^2 = Y^2 \qquad (12)$$

with Y given by Eq.(3). The quadratic yield surface Eq.(12) displays a shear yield strength almost equal to the normal tensile (or compressive) strength for the typical value $\alpha \approx 2$.

The collapse locus for a sandwich core comprising tetrahedral struts or pyramidal struts can be calculated by plastic collapse theory; the geometry of these lattice materials is sketched in Fig. 6. We suppose that the face sheets of the sandwich panel are separated by circular cylindrical struts of radius a and length ℓ, with each strut inclined at an angle ω to the face sheet. For the case of an octet-truss architecture the angle ω is given by $\cos\omega = 1/\sqrt{3}$. The nodes of the face sheets are arranged on a hexagonal grid for the tetrahedral core, and on a square grid for the pyramidal core. In contrast to the metallic foam core, the lattice core is not transversely isotropic and the transverse shear strength varies with orientation. Collapse calculations [7] reveal that the minimum transverse shear strength is achieved for the macroscopic loading direction σ_{12} for both architectures, in the axes shown in Fig. 6.

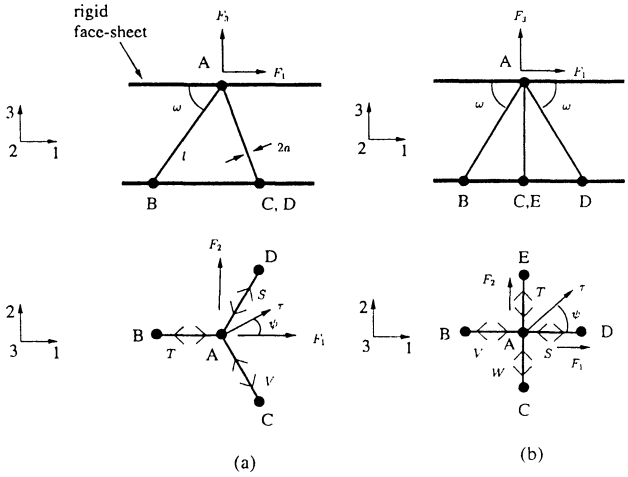

Fig. 6. Geometry of the (a) tetrahedral core and (b) pyramidal core. (S,T,V) are the bar tensions of the tetrahedral truss and (S,T,V,W) are the bar tensions of the pyramidal truss due to a nodal load $\boldsymbol{F}$ applied to node A of each assembly.

Consequently, we explore here the collapse state for the combined loading $(\sigma_{33}, \sigma_{13})$ on the faces of the sandwich panel. Consider first the tetrahedral core. The collapse locus consists of a series of straight lines in $(\sigma_{33}, \sigma_{13})$ loading space, corresponding to yield of the bar AB, or combined yield of bars AC and AD of Fig. 6a. The yield surface is defined by

$$\frac{2}{\cos\omega}\frac{\sigma_{13}}{\sigma_Y} + \frac{1}{\sin\omega}\frac{\sigma_{33}}{\sigma_Y} = \pm\bar{\rho}\sin\omega \qquad (13a)$$

and

$$-\frac{1}{\cos\omega}\frac{\sigma_{13}}{\sigma_Y} + \frac{1}{\sin\omega}\frac{\sigma_{33}}{\sigma_Y} = \pm\bar{\rho}\sin\omega \qquad (13b)$$

where $\bar{\rho}$ is again the relative density of the core. For the case of the pyramidal core, plastic collapse is either by bars AB and AD undergoing simultaneous yield, or bars AC and AE undergoing simultaneous yield, giving

$$\frac{|\sigma_{13}|}{\sigma_Y} = \frac{1}{4}\bar{\rho}\sin 2\omega \qquad (14a)$$

and

$$\frac{|\sigma_{33}|}{\sigma_Y} = \bar{\rho}\sin^2\omega \qquad (14b)$$

These yield surfaces are sketched in Fig. 7. We note that the shear yield strength and transverse strength for the tetrahedral lattice have identical respective values to those for the pyramidal lattice. However, the shapes of the yield surface are different, with the pyramidal geometry giving the greater strengths in the first and third quadrants. We conclude that the pyramidal microstructure is preferred, with a maximum value of specific shear strength achieved at $\omega = \pi / 4$. As noted above, the multi-axial strength of the lattice core is significantly greater than that of the metallic foam core since the strength of the lattice material scales linearly with $\overline{\rho}$, while the strength of the metallic foam scales as $\overline{\rho}^{3/2}$.

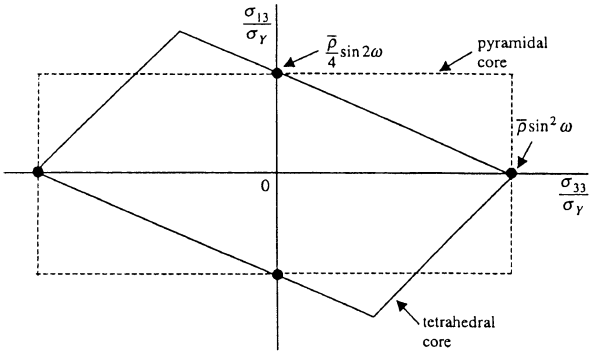

Fig. 7. Sketch of the collapse surface for lattice cores of tetrahedral and pyramidal architectures.

5. CONCLUSIONS

Periodic lattice materials can be designed to possess higher stiffnesses and strengths than stochastic foams by selecting a topology of adequate connectivity (at least 12 for a similarly situated 3D structure). A simple but adequate phenomenological model has been developed for the yielding of metallic foams, and isotropic hardening appears to be an adequate description of the hardening behaviour. The lattice material of octet truss architecture is a redundant structure, and fails by a number of competing collapse modes under multi-axial loading.

Acknowledgements – The author is grateful for continued collaborations with V. S. Deshpande, C. Chen, T. J. Lu and M. F. Ashby at Cambridge University, with A. G. Evans at Princeton University and J. W. Hutchinson at Harvard University.

REFERENCES

1. M.F. Ashby, A.G. Evans, N.A. Fleck, L.J. Gibson, J.W. Hutchinson and H.N.G. Wadley, Metal Foams - A Design Guide, Butterworth-Heinemann Boston, USA (2000).
2. V.S. Deshpande, N.A. Fleck, J. Mech. Phys. Solids, 48 (2000) 1253.
3. C. Chen, T.J. Lu and N.A. Fleck, J. Mech. Phys. Solids, 47 (1999) 2235.
4. C. Chen, Technical Report CUED /C-MICROMECH/ TR.20, April 1999, Cambridge University Engineering Department, Trumpington Street, Cambridge CB2 1PZ, UK.
5. V.S. Deshpande, M.F. Ashby and N.A. Fleck, to appear in Acta Materialia (2001).
6. V.S. Deshpande, N.A. Fleck and M.F. Ashby, to appear in J. Mech. Phys. Solids (2001).
7. V.S. Deshpande and N.A. Fleck, submitted to Int. J. Solids and Structures (2001).